

## **Pitfalls in the Evaluation of X-ray Diffraction Line Shape\***

*Gerhard Zorn*

Siemens AG, Corporate Research and Development,  
Otto-Hahn Ring 6, D-8000 Munich, West Germany.

### *Abstract*

The sources of errors in the analysis of X-ray diffraction profiles are described, and recipes are given to minimise or eliminate these errors. It is proposed that a sample at high temperatures is used as a standard. The influence of measurement statistics on the Fourier transform of deconvoluted functions is demonstrated through computer simulations. The necessity for smoothing procedures is stressed. It is shown how the parameter step width, number of sampling points, and position of origin for the Fourier transformation can be optimised, and thus a reliable basis can be created for the interpretation of the Fourier transform in terms of crystallite size, size distribution, and microstrain.

### **1. Introduction**

Peak width analysis and peak profile analysis have become established methods to analyse crystallite size, crystallite size distribution, and microstrain in powder samples or in polycrystalline thin films. Among many various procedures which have been developed to extract these parameters from measured peak profiles, the so-called Fourier methods form an essential part. The most commonly known Fourier method is the one described by Warren and Averbach (1952) and Warren (1959) which uses multiple lines. The other Fourier methods are single line methods (Pines and Sirenko 1962; Gangulee 1974; Mignot and Rondot 1975).

This paper describes, after a review of the procedures mentioned has been given, how errors affect the results of profile analysis. Recipes are given on how these errors can be avoided or their effects can be minimised.

### **2. Procedures in Fourier Methods**

For evaluations employing any of the procedures mentioned, one needs the Fourier transform  $F(n)$  of the pure broadening function  $f(x)$  of the sample which is generally gained by employing the Stokes (1938) correction. This requires the measurement of the broadened sample profile  $h(x)$  and of a standard profile  $g(x)$ , where  $g(x)$  is

\* Paper presented at the International Symposium on X-ray Powder Diffractometry, held at Fremantle, Australia, 20–23 August 1987.

characteristic for the diffractometer at a certain diffraction angle and for the spectral distribution of the radiation used at this angle:

$$F(n) = H(n)/G(n), \quad (1)$$

where  $H(n)$  and  $G(n)$  are the Fourier transforms of the sample profile and standard profile respectively.

(a) *Warren-Averbach Method*

According to Warren and Averbach (1952), the real part of the Fourier transform of a broadening function can be split into an order dependent and an order independent term describing an average column length in crystallites and microstrain:

$$A(n) = A(n)^{\text{size}} A(n)^{\text{strain}}, \quad (2)$$

where

$$A(n)^{\text{size}} = \frac{N_n}{N_3} = \frac{1}{N_3} \int_{i=n}^{\infty} (i-n) p_i \, di, \quad (3)$$

$$A(n)^{\text{strain}} = \langle \cos\{2\pi l Z(n)\} \rangle. \quad (4)$$

Here  $N_n$  is the average number of unit cell pairs along a crystallite chord, where the cells forming a pair are  $n$  unit cells apart. This average  $N_n$  can also be expressed in terms of a column length distribution, where  $p_i \, di$  is the fraction of columns with a length between  $i$  and  $i+di$  cells (Bertaut 1950; Warren 1959). The order of a reflection is denoted by  $l$ , and  $Z(n)$  is the absolute displacement in unit cells of two cells which are  $n$  cells apart. Later a quantity  $\epsilon(n)$  will be introduced, which stands for a relative distortion [ $\epsilon(n) = Z(n)/n$ ]. For the separation of size and strain, we make use of the fact that  $A(n)^{\text{size}}$  is independent of  $l$ , while  $A(n)^{\text{strain}}$  is not:

$$\begin{aligned} \ln A(n) &= \ln A(n)^{\text{size}} + \ln A(n)^{\text{strain}} \\ &= \ln A(n)^{\text{size}} + \ln \langle \cos\{2\pi l \epsilon(n) n\} \rangle. \end{aligned} \quad (5)$$

The cosine and the logarithm of the second term are expanded leading to

$$\ln A(n) = \ln A(n)^{\text{size}} - 2\pi^2 l^2 \langle \epsilon(n)^2 \rangle n^2. \quad (6)$$

The slopes of graphs of  $\ln A(n)$  as a function of  $l^2$  for every  $n$  yield therefore values for the microstrain  $\langle \epsilon(n)^2 \rangle$ . The intercepts yield values for  $\ln A(n)^{\text{size}}$ . From these one can calculate an average column length by using

$$\frac{dA(n)^{\text{size}}}{dn} = -\frac{1}{N_3} \int_{i=n}^{\infty} p_i \, di = -\frac{1}{N_3} \quad \text{for } n \rightarrow 0, \quad (7)$$

and the column length distribution

$$\frac{d^2 A(n)^{\text{size}}}{dn^2} = \frac{p_n}{N_3}. \quad (8)$$

### (b) Single Line Evaluations

Most schemes in single line evaluations start with the assumption that particle size causes peak broadening in the shape of a Lorentzian curve, while microstrains broaden a peak to Gaussian shape. The measured peak is then a convolution of both shapes. It is possible to separate the two effects using the Fourier transform of the broadening function:

$$A(n) = A(n)^{\text{Lorentz}} A(n)^{\text{Gauss}} = e^{-an} e^{-bn^2}. \quad (9)$$

The contributions from both functions can be separated again by taking the logarithm

$$\ln A(n) = -an - bn^2 = -\frac{n}{N_3} - 2\pi^2 l^2 \langle \epsilon^2 \rangle n^2, \quad (10)$$

where  $\langle \epsilon^2 \rangle$  is an average strain independent of  $n$ . Equation (10) is then a second degree polynomial. The coefficients can be evaluated with, for example, a least-squares fit. This replacement of  $A(n)^{\text{Gauss}}$  by  $\exp(-2\pi^2 l^2 \langle \epsilon^2 \rangle n^2)$  is equivalent to the Warren (1959) expression for  $A(n)^{\text{strain}}$ . It is allowed if the strain distribution is assumed to be Gaussian and not dependent on  $n$ , because the Fourier transform of a Gaussian curve is a Gaussian curve again.

The replacement of  $\ln A(n)^{\text{Lorentz}}$  by  $-n/N_3$  can be explained by assuming that the sample contains only columns with a single length of  $i$  cells. Then the integral over the column length distribution function (7) is always equal to 1 if  $n \leq i$ . The slope of the  $A(n)^{\text{size}}$  curve is therefore constant and equal to  $-1/N_3$ . Since  $A(0)$  is normalised to 1, the equation for the curve is  $A(n)^{\text{size}} = 1 - n/N_3$  and  $\ln A(n)^{\text{size}} = -n/N_3$  for small  $n/N_3$ .

This method described is similar to a non-Fourier method which uses the Voigt function (de Keijser *et al.* 1982), a convolution of Lorentzian and Gaussian curves, to separate size and strain effects. The results of both methods are, however, not directly comparable (Delhez *et al.* 1982). In contrast to the single line method described, other procedures do assume that strain is a function of  $n$  (Gangulee 1974; Mignot and Rondot 1975). This assumption is probably closer to reality. Most often strains are assumed to decrease with  $1/n$  (Rothman and Cohen 1969). Equation (9) becomes then, after an expansion of the exponential function,

$$A(n) = (1 - an)(1 - cn). \quad (11)$$

The coefficients are then evaluated from pairs of Fourier coefficients or from least-squares fits of the whole curve.

## 3. Errors in Profile Analysis and Recipes for Minimising Them

### (a) Designing the Experiment—Choice of a Standard Material

In designing the experiment, one should try to eliminate as many sources of errors as possible. This begins with the selection of peaks, and of the radiation used. Peaks with as little overlap as possible should be selected. By choosing a suitable wavelength they can be shifted to diffraction angles where broadening effects can be detected with more accuracy. The use of an incident beam monochromator eliminates the need to correct for  $K\alpha_2$  radiation. Powder samples have to be prepared carefully concerning

geometry and packing density (for thin films, these two parameters can easily be kept constant). The biggest problem is, however, the choice of a standard material.

The Stokes correction (1) requires the measurement of a standard which does not exhibit any line broadening due to sample properties, and which, in the ideal case, is the same material as the sample. An ideal standard is practically never available. Non-ideal standards often have different transparency, geometry (thickness, dimensions, packing density), and show peaks at different diffraction angles compared with the sample. If particle size in a standard is too large, its peaks will be composed of a small number of peaks from these large crystallites. This peak is then much narrower than an ideal standard peak and contains structure which a peak from an ideal powder sample would not show. Strong texture, which occurs for example in thin films, also influences peak shape.

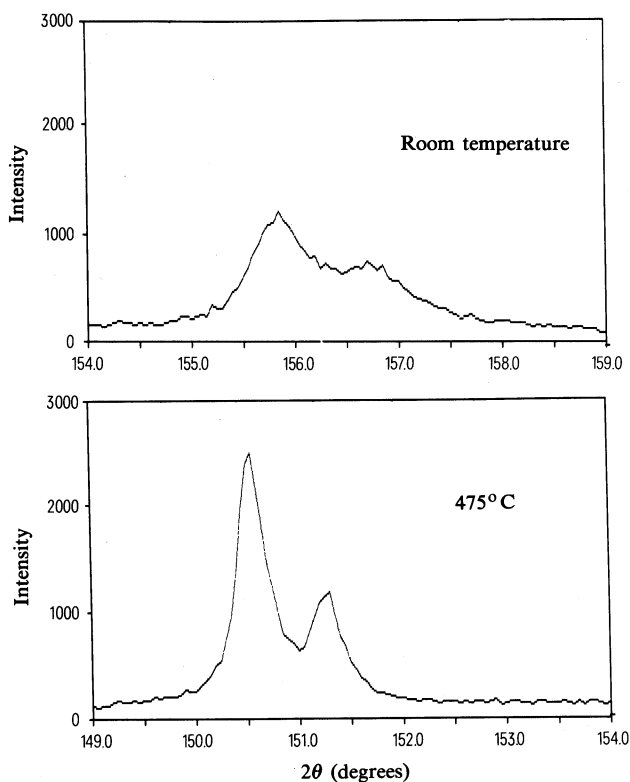


Fig. 1. The 222 reflection of an Al(1%Ti) thin film measured with Cr radiation at room temperature and at 475°C. The peak at room temperature is broadened by microstrain. The strain relaxes at high temperatures.

Several papers have been published which describe the effects of non-ideal standards in profile analysis and show how these errors can be minimised (de Keijser *et al.* 1978; Delhez *et al.* 1979). This paper describes a method for producing an almost ideal standard. Here the sample at high temperatures is used as its own standard. It is known that crystallites grow at high temperatures and that defects can be

annealed. It is also known that high temperature affects a peak profile only slightly. The Debye–Waller factor contains a  $\sin\theta$  term which describes the influence of temperature on a diffraction profile. This influence, however, is only noticeable over a large range of  $\sin\theta$ . The peaks used for standards in profile analysis are supposed to be narrow, so their profile stays practically unchanged. The advantage of this method is that transparency and geometry of the standard are very close to that of the sample. The disadvantage is that the method can be applied only to selected materials whose particles actually grow to sufficient size or whose strains disappear at high temperatures. Figs 1 and 2 show two examples where the high temperature standard could be applied. Fig. 1 shows the  $K\alpha_1$ – $\alpha_2$  doublet of the 222 reflection (Cr radiation) of an Al layer (doped with Ti) at room temperature and at 475°C. The peak at room temperature is broadened by microstrain. This broadening disappears at high temperature and returns after cooling, so the peak at high temperature is therefore close to a low strain state. Temperature expansion and the relaxation of macrostrains (Göbel 1986) shift the position of the peak, so that it does not represent an ideal standard in this point. On a  $\sin\theta$  scale this effect seems to be negligible though. The second example (Fig. 2) shows a high temperature measurement of ZnO powder. At room temperature the sample has a crystallite size of approximately 5 nm. At high temperatures, the crystallites start to grow and the peaks become narrower. Instead of using a separate measurement of annealed ZnO powder as a standard, a measurement of the sample at high temperature after sufficient annealing time is used as a standard. The problem of having to prepare an identical powder sample for a standard measurement has thus been eliminated.

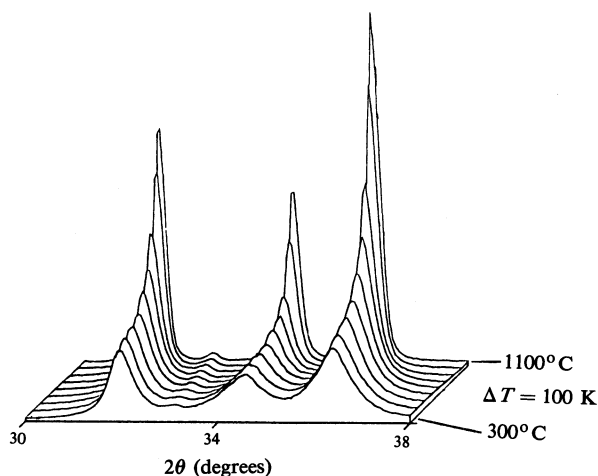
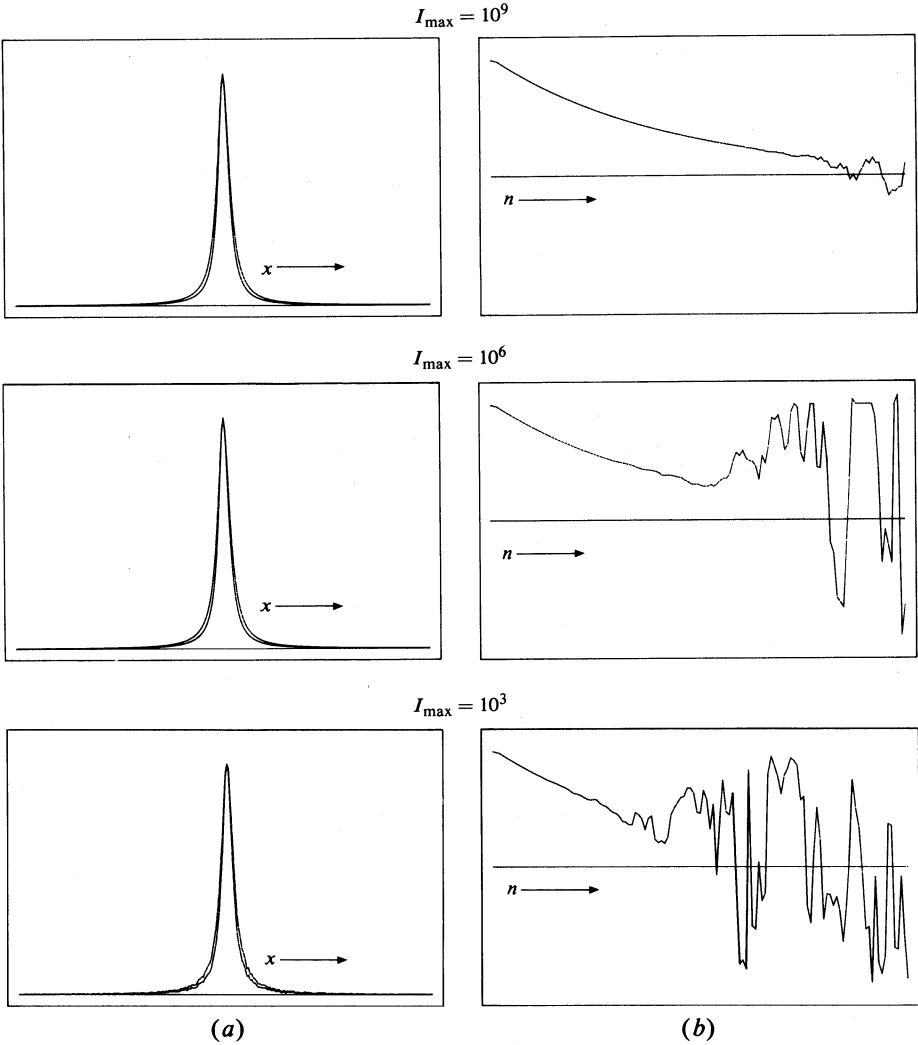


Fig. 2. High temperature measurement of ZnO powder between 300°C and 1100°C. The peaks at high temperature become narrower due to the growth of particles.

#### *(b) Measurement Statistics and the Application of Smoothing Procedures*

One of the most serious errors which can be made in profile analysis is using data for profile evaluations which are just sufficient for phase identification. Profile analysis requires definitely better counting statistics.



**Fig. 3.** (a) Lorentzian functions with various maximum intensities and superimposed statistics (256 points and coordinate  $x$  in real space). (b) Real part of the Fourier transform of the deconvoluted curves from (a) (coordinate  $n$  in reciprocal space).

The effect of poor counting statistics on the Fourier transform of a deconvoluted function and on the results of profile analysis will be shown by computer simulations. A Lorentzian function of  $0.15^\circ$  full width at half maximum (FWHM) was chosen to represent a standard profile. The broadening of the sample profile was assumed to be 20%, leading to a Lorentzian function with  $\text{FWHM} = 0.18^\circ$ . The profiles were sampled at 256 points, the sampling interval being  $0.02^\circ$ . The profiles were then superimposed by artificial statistics. Sample and standard profiles with various maximum intensity  $I_{\max}$  are shown in Fig. 3a. The Fourier transforms of the pure broadening functions were calculated with a fast Fourier transform algorithm (Brigham 1974) and are displayed in Fig. 3b. The imaginary part of the functions is zero because the symmetrical functions were transformed with the maximum being the origin for transformation.

The upper part of Fig. 3, representing the best statistics ( $I_{\max} = 10^9$ ), shows a smooth decrease of the real Fourier coefficients  $A(n)$ . At large values of  $n$  the Fourier transform of the deconvoluted curve begins to show erratic oscillations. This is due to the finite range effect (Young *et al.* 1967) which causes small oscillations on the  $A(n)$  curve that are of the order of  $A(n)$  for high values of  $n$  in Fig. 3. The limited precision of computer calculated numbers and measurement statistics contribute to this effect. By applying the deconvolution theorem (1) (which means division by a small number that fluctuates erratically around zero) the small oscillations in the Fourier transforms of both functions become suddenly obvious.

If one examines the peaks in the middle of Fig. 3 ( $I_{\max} = 10^6$ ), one finds erratic oscillations at much lower values of  $n$ . These again were enlarged by the division which is applied to calculate the deconvoluted Fourier transform. This happens although the statistics added to the pure profiles cannot be detected by eye. The peaks at the bottom of Fig. 3 ( $I_{\max} = 10^3$ ) display this effect even more, although to the eye the statistics may still look sufficiently good. Even the starting values of  $A(n)$  have been affected. This effect is even more obvious if one approaches the limits of detection of peak broadening. If the Fourier transforms of the two profiles are close to each other, the errors described start at very low values of  $n$ .

All this has serious consequences for the following steps of analysis. If one positions the peaks from this example at for example  $40^\circ 2\theta$ , applies Cu  $K\alpha_1$  radiation for the following calculations, and assumes that only particle size broadened the peak, one finds an average column length of 99 nm for smooth peaks. The peaks with a maximum intensity of  $10^3$ , however, showed in a number of evaluations fluctuations of the particle size between 93 and 105 nm, i.e. of the order of 5%. For the peaks with  $I_{\max} = 10^6$  the effect is still present, the particle size varying between 98 and 100 nm. For the maximum intensity of  $10^9$  the evaluated particle size is finally constant.

If these findings are applied not only to a particle size evaluation but to a complete Warren-Averbach analysis, one can conclude that an evaluation of a strain curve according to equation (6) becomes almost impossible with raw data. The number  $n$  of valid strain values will be quite limited by the early starting spurious oscillations. Physically impossible negative values for  $\langle \epsilon(n)^2 \rangle$  will appear. The errors in the  $A(n)^{\text{size}}$  which are then found by extrapolation of (6) will be even more pronounced than in pure crystallite size evaluations. Concerning the column length distributions (8), it is obvious that the second derivative of the shown Fourier transforms with erratic oscillations will not yield any physical information.

The errors described can fortunately be minimised by applying smoothing procedures to the measured profiles. In addition to the application of simple smoothing procedures, smoothing can also be done by least-squares fits of measured data with analytical functions. This has the advantage of performing background subtraction and  $K\alpha_2$  correction (if necessary) at the same time. Peaks can be extracted from superpositions and intensities can be recalculated at any value on a  $\sin\theta$  scale. The disadvantage of this method is that by forcing simple profiles like Gaussian or Lorentzian curves on the measured data, some of the information in the measurement is lost. A 'bendable' function such as the split Pearson VII function is better suited to approximate a measured profile.

It must not be forgotten, however, that smoothing does not yield an unambiguous result. Depending on the counting statistics, smoothing yields a bandwidth of possible solutions in the measured range of a profile, with the band being narrower the

better the statistics. If the desired profile has, for example, been extracted from a superposition of peaks, or if a profile is extrapolated far into the tails of a peak (this is necessary to minimise the finite range effect), these extrapolated values differ more from the 'true' values if they were extrapolated from a broad band of possible smoothing solutions.

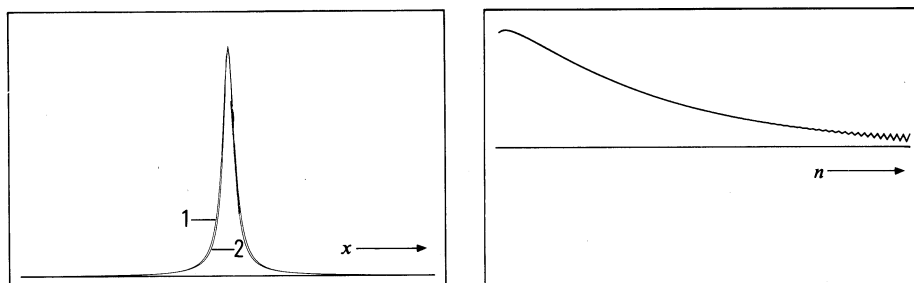


Fig. 4. Creation of a hook effect in the Fourier transform of a deconvoluted function by an incorrect extrapolation of the measured profiles.

Among the commonly known analytical functions, the split Pearson VII functions yield the best smoothing results. A danger existing lies in the correlation between FWHM and exponent in the Pearson VII function. A bandwidth of combinations of FWHMs and exponents fit a peak equally well. Extrapolation from the fitted range into the tails of a peak depends, however, strongly on the exponent. Errors may arise especially with small peak broadenings. Fig. 4 shows two symmetrical Pearson VII functions ( $\text{FWHM}_{\text{sample}} = 0.18^\circ$ ,  $\text{exp}_{\text{sample}} = 1.0$  and  $\text{FWHM}_{\text{standard}} = 0.15^\circ$ ,  $\text{exp}_{\text{standard}} = 0.9$ ). The Fourier transform of the deconvoluted function shows a large hook effect. This means that the standard curve 2, although it looks narrower to the eye than the sample curve 1 at for example half height, is actually broader than the sample curve in the tails of the peaks. Theory requires, however, that peaks are broadened symmetrically, i.e. that the sample peak is broader than the standard peak over its whole extrapolated range. In practice this possible error can be eliminated by making sure that a least-squares fit program selects from the band of combinations of FWHMs and exponents the one solution that describes the standard peak with higher exponents than the sample peak (a curve with a high exponent falls faster to zero than a curve with low exponent). The sample curve then always lies above the standard curve. This procedure does not solve the problem of extrapolation but it excludes a physical impossibility. One could also use fitted data only in the range they were measured in, and extrapolate with other procedures which have more physical meaning (Delhez *et al.* 1986).

### (c) Fourier Transformation and Stokes Correction

The calculation of Fourier transforms is usually done with sampling points equidistant on a  $\sin\theta$  scale which is equivalent to a linear reciprocal length scale. This requires the calculation or interpolation of sampling points from reduced data (e.g. least-squares fit results or spline functions). Corrections of the profile according to the Lorentz factor, polarisation factor, and Debye-Waller factor can be included here.

By using fast Fourier transform algorithms, modern computers can do a Fourier transformation on a large number of sampling points virtually instantaneously. If one



uses an algorithm for complex functions, one can transform sample peak and standard peak at the same time (independent of the sampling interval on each peak). Since the measured profiles are real values and contain no imaginary part, one can store the two functions in the real part and in the imaginary part, respectively, of the complex function to be transformed. The Fourier transforms of the two measured profiles can be extracted from the Fourier transform of the complex function (Brigham 1974). The computation time for the two necessary Fourier transformations (per peak used in the evaluation) can thus be cut by half.

Several parameters have to be optimised for the Fourier transformation to avoid errors which can hardly be corrected later. Of importance are three parameters, namely sampling interval on the measured profile, number of sampling points (these two determine the range for transformation), and position of origin for the Fourier transformation. What one would like to have for the interpretation in terms of size, size distribution, and strain is a smooth curve with small sampling interval and physically valid values up to high harmonic numbers  $n$ . In the ideal case, this Fourier transform does not contain any imaginary part, and the real part is larger than zero over its whole range.

The effect of using a finite range for transformation has been mentioned already. It results in a convolution of the Fourier transform of the sample broadening function with the Fourier transform of a slit function. The larger the range which is used for transformation, the narrower the function

$$\text{FT}^{\text{slit}} = S(n) = \sin(\pi nx)/\pi n, \quad (12)$$

and the less is its influence on the true profile  $H(n)$  in the convolution

$$H(n) = H_{\infty}(n) S(n). \quad (13)$$

Therefore, to minimise the effect of finite range, the measured peak should be narrow compared with the range in which it is sampled. This is the reason why a profile should be extrapolated into the tails.

**Table 1.** Number of sampling points above half height of a peak necessary to avoid aliasing of the Fourier transform

$A(n)$	Lorentzian	Modified Lorentzian	Gaussian
$10^{-2} A(0)$	5	4	4
$10^{-3} A(0)$	5	5	4
$10^{-4} A(0)$	6	5	5
$10^{-5} A(0)$	8	7	5
$10^{-6} A(0)$	10	9	6

A large range for transformation can be achieved by either a large sampling interval, by a large number of sampling points or by both. The sampling theorem (Brigham 1974) states that sampling of a profile at intervals  $x$  causes a periodicity in the Fourier transform with the period being  $1/x$ . The Fourier transform of the profile is thus repeated every  $1/x$ . If the Fourier transform of a profile has not fallen

to practically zero after  $1/2x$ , the  $A(n)$  at high values of  $n$  will be erroneous due to overlap with the peak of the next period. This phenomenon is called aliasing. To avoid aliasing, the sampling interval on the measured profile must therefore be small. How small it has to be cannot be stated in absolute units. The user has to define a lower limit for  $A(n)$ , e.g.  $A(n) = 10^{-5} A(0)$ , where the limit depends on the accuracy of the computer calculations. From this, one can calculate a relation between FWHM of a certain peak shape and the sampling interval of the peak (Young *et al.* 1967). The problem of determining the best sampling interval is thus reduced to sampling in a way which puts a certain number of points above half the height of the peak. Table 1 gives these numbers calculated for Lorentzian, modified Lorentzian (Pearson VII with exponent 2), and Gaussian curves for various low limits of  $A(n)$ .

This result also shows how to minimise the finite slit effect. At an optimised sampling interval, the number of sampling points has to be increased. This increase of the transformed range also has the positive effect that the sampling interval of the Fourier transform decreases correspondingly. This means that the following interpretation of the  $A(n)$  can be done with fine spaced values. A small sampling interval is also important for another reason. Young *et al.* (1967) showed that a residual constant background on a profile affects  $A(0)$  but does not change the other  $A(n)$ . Also, the necessary truncation affects  $A(0)$  which describes the area of a peak. It is therefore desirable to evaluate values as close to  $A(0)$  as possible which can be gained by using a small interval.

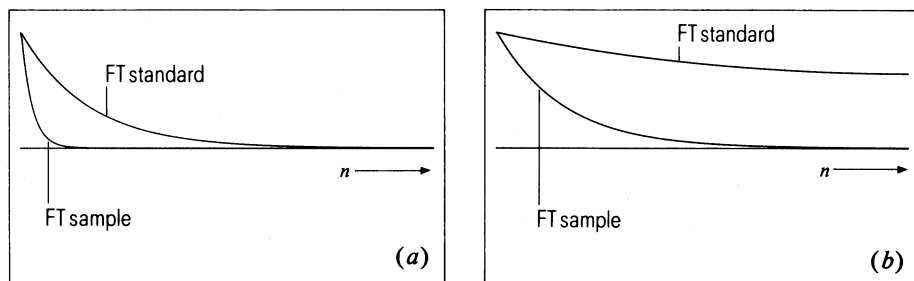


Fig. 5. Fourier transform of standard peak and sample peak: (a) with step width optimised for the standard peak and (b) with step width optimised for the sample peak.

After standard peak and sample peak have been Fourier transformed, the Stokes correction has to be applied. Here a problem arises if both peaks had largely different width and were transformed with the same step width. If the step width was optimised for the standard peak (see Fig. 5a), the Fourier transform of the sample peak will fall to zero quickly (no aliasing but only few values that can be used for the evaluation). The  $A(n)$  at high  $n$  will be superimposed by statistical fluctuations originating in computation errors, and by regular oscillations originating in the finite range. The curve will, in addition, be broadened considerably by the convolution with the Fourier transform of the slit function. If the step width, on the other hand, is optimised for the sample profile (Fig. 5b), the Fourier transform of the standard will be aliased. This is not a very critical problem as long as moderate peak broadenings are involved and as long as no evaluations of size distribution functions are planned where accurate

$A(n)$  at high  $n$  are needed. If peak broadening is very large, aliasing will however heavily affect all values of the standard's Fourier transform. The problem can be solved by optimising step widths for both sample and standard profile. The sampling interval for the sample peak will be larger than for the standard peak, since the sample peak is always broader than the standard peak. If the number of sampling points is equal for sample and standard, the sampling interval of the Fourier transforms will therefore be smaller for the sample. The correct  $A(n)$  of the standard can then be found by interpolation at the interval that was calculated for the sample.

Applied to multiple line analysis, one can conclude that each peak requires its own step width. The Fourier interval for the adjacent steps of evaluation is best chosen from the Fourier interval of the broadest sample peak. The Fourier transforms of all other peaks can then be interpolated at this sampling interval.

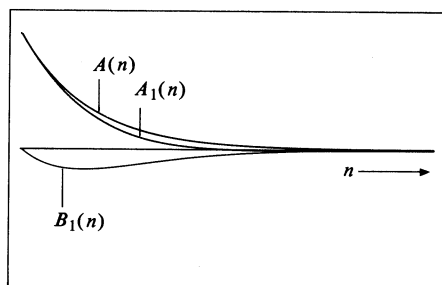


Fig. 6. Fourier transform of a symmetrical function. For  $A(n)$  the origin for transformation coincides with the symmetry axis of the profile, while  $A_1(n)$  and  $B_1(n)$  are the real and imaginary parts with the origin for transformation shifted by  $(1/1024)2\pi$ .

The choice of origin for the Fourier transformation is of great importance for the results in profile analysis. If  $h(x)$  is a peak profile whose Fourier transform is  $H(n)$ , and  $h_1(x)$  is the same profile shifted by  $x_0$  relative to the origin used for the transformation of  $h(x)$ , the Fourier transform of  $h_1(x)$  can be written as

$$\begin{aligned}
 H_1(n) &= A_1(n) + i B_1(n) \\
 &= \{A(n) + i B(n)\} \exp(2\pi i x_0 n) \\
 &= A(n) \cos(2\pi x_0 n) - B(n) \sin(2\pi x_0 n) \\
 &\quad + i \{A(n) \sin(2\pi x_0 n) + B(n) \cos(2\pi x_0 n)\}, \tag{14}
 \end{aligned}$$

$$A_1(n) = A(n) \cos(2\pi x_0 n) - B(n) \sin(2\pi x_0 n), \tag{15}$$

$$B_1(n) = A(n) \sin(2\pi x_0 n) + B(n) \cos(2\pi x_0 n), \tag{16}$$

where  $A_1(n)$  and  $B_1(n)$  are real and imaginary part of the shifted function  $h_1(x)$ , and  $A(n)$  and  $B(n)$  are for the unshifted function. According to Warren and Averbach (1952) only symmetrical broadenings are treated. Asymmetries in the measured profiles are supposed to be properties of the diffractometer (i.e. the sample profile is asymmetric because the standard profile is asymmetric). The deconvolution of both measured profiles leads according to theory to a symmetrical profile which may, however, be shifted relative to its symmetry axis. This happens because the origins of the two measured functions are not fixed, but are chosen for example at their

maximum. If the pure broadening function is symmetrical, its imaginary part  $B(n)$  in (15) and (16) is zero. In this case the shift  $x_0$  of the broadening function  $h_1(x)$  can be determined from the slope of the  $B_1(n)$  for  $n \rightarrow 0$  in (16) (Delhez *et al.* 1979; de Keijser *et al.* 1980). With this value, the  $A(n)$  for the unshifted function  $h(x)$  can be reestablished according to (15). This method is of limited accuracy since the slope of  $B_1(n)$  for  $n \rightarrow 0$  cannot be determined accurately. The error becomes smaller with decreasing interval of the Fourier transform. If the Fourier coefficients of the shifted function are used for further evaluations (Warren–Averbach or single line), large errors result. The  $A_1(n)$  of the shifted function are generally smaller than the  $A(n)$  of the unshifted function (see Fig. 6). This will lead to erroneous strain values, depending on which peak in the analysis was displaced (equation 6). The extrapolated  $A(n)^{\text{size}}$  values will in accordance be also erroneous. Equation (15) shows that  $A_1(n)$  will be negative for certain combinations of  $x_0$  and  $n$ . This limits the number of values of  $n$  that can be used for the evaluation of (5). In practice it often happens that the function  $h(x)$  is not symmetrical, although it is supposed to be. In this case an iterative procedure can be applied which varies  $x_0$  and searches for a minimum for  $\Sigma |B_1(n)|$ . With this  $x_0$  one can again reestablish the  $A_1(n)$ . Another method to handle asymmetric or displaced functions is described in the review article by Delhez *et al.* (1982).

#### 4. Conclusions

Many errors in Fourier methods do occur before the Fourier transform of the broadening function is actually interpreted in terms of crystallite size, size distribution and microstrain. Errors can be made in designing and performing the measurement, and in calculating the Fourier transform of the pure broadening function. This paper showed how these errors can be minimised or eliminated, and thus a good basis for the various evaluation methods can be created. This does, however, not yet guarantee reliable results. There are limitations and approximations inherent in the evaluation methods described in Section 1 (de Keijser *et al.* 1977; Delhez and Mittemeijer 1976). Also the theoretical models with their assumptions as the basis for these methods do not necessarily meet reality. Results are expressed in terms of parameters like column length distributions or root-mean-square strain which cannot readily be compared with more understandable parameters. Although this problem exists, profile analysis can give comparable results which describe the state of strain in a sample and give an impression of the crystallite sizes present.

#### References

- Bertaut, F. (1950). *Acta Cryst.* 3, 14–18.
- Brigham, E. O. (1974). 'The Fast Fourier Transform' (Prentice Hall: New York).
- de Keijser, Th.H., Langford, J. I., Mittemeijer, E. J., and Vogels, A. B. P. (1982). *J. Appl. Cryst.* 15, 308–14.
- de Keijser, Th.H., and Mittemeijer, E. J. (1977). *Philos. Mag.* 36, 1261–4.
- de Keijser, Th.H., and Mittemeijer, E. J. (1978). *Z. Naturforsch.* 33, 316–20.
- de Keijser, Th.H., and Mittemeijer, E. J. (1980). *J. Appl. Cryst.* 13, 74–7.
- Delhez, R., de Keijser, Th.H., and Mittemeijer, E. J. (1979). Proc. Symp. on Accuracy in Powder Diffraction, NBS Publ. No. 567, pp. 213–53 (NBS: Gaithersburg).
- Delhez, R., de Keijser, Th.H., and Mittemeijer, E. J. (1982). *Fresenius Z. Anal. Chem.* 312, 1–16.
- Delhez, R., de Keijser, Th.H., and Mittemeijer, E. J. (1986). *J. Appl. Cryst.* 19, 459–66.
- Delhez, R., and Mittemeijer, E. J. (1976). *J. Appl. Cryst.* 9, 233–4.

- Gangulee, A. (1974). *J. Appl. Cryst.* **7**, 434–9.
- Göbel, H. E. (1986). Proc. Int. Conf. on Residual Stresses (Eds E. Macheranch and U. Hank), pp. 501–8 (Garmisch-Partenkirchen).
- Mignot, J., and Rondot, D. (1975). *Acta Metall.* **23**, 1321–4.
- Pines, B. Y., and Sirenko, A. F. (1962). *Sov. Phys. Cryst.* **7**, 15–21.
- Rothman, R. L., and Cohen, J. B. (1969). *Adv. X-Ray Anal.* **22**, 208–35.
- Stokes, A. R. (1938). *Proc. Phys. Soc. London* **61**, 382–91.
- Warren, B. E. (1959). *Prog. Met. Phys.* **8**, 147–202.
- Warren, B. E., and Averbach, B. L. (1952). *J. Appl. Phys.* **23**, 497.
- Young, R. A., Gerdes, R. J., and Wilson, A. J. C. (1967). *Acta Cryst.* **22**, 155–62.

Manuscript received 21 August, accepted 11 December 1987

